the trichloride, less for the tribromide, and negligible for the iodides. Alternatively we have calculated an experimental effective Zr^{3+} radius and compared it to the octahedral hole size calculated for an idealized hard-sphere model (Table V). In the chloride case the fit is good, while in the iodide case the site radius is almost 25% larger than the metal atom radius. For this series of zirconium halides a 3% excess in the site radius over the metal ion radius results in a 5% elongation of the metal–metal distance over the ideal interhole distance in the chloride; in the bromide an 11% excess in site radius results in a 2% elongation, and in the iodide a 25% excess in the site radius results in no elongation.

Consideration of the rms thermal displacements (Table III) reveals that the distribution of the metal atom electron density becomes progressively more elongated along the *c* axis in the series even though the site radius increases in size symmetrically. It appears that the metal ions with high formal charges compared to the counterion in an anisotropic structure require more space in the direction of the anisotropy to minimize nearest-neighbor metal ion repulsions. On the other hand, minimal oscillation is required perpendicular to the direction of structural anisotropy due to the lack of nearest-neighbor metal atoms at sufficiently short distances. A similar elongation of metal atom occupied octahedra has been observed by Magneli[30] along the *b* axis of the monoclinic homologous series M_nO_{3n-1} and M_nO_{3n-2} (M = Mo, W). If the zirconium trihalides are viewed as Magneli-type phases, the elongation of the octahedra is the result of the distortion necessary to reduce repulsive nearest-neighbor metal ion interactions when excess metal ion site radius is unavailable. However, the fact that distortion occurs does not necessarily totally eliminate bonding interactions between the d^1 electrons of the zirconiums, because the magnitude of the distortion must be the resultant of the repulsive electrostatic forces and the attractive bonding forces. It does seem clear that the d^1 electrons enter into a more complex behavior than simple σ-bond formation, as evidenced by the field-dependent, temperature-independent paramagnetism of the trihalides[31] and the valence photoelectron emission spectra[32] of the trichloride.

Acknowledgment. This work was supported in part by the Research Committee of the Graduate School from funds supplied by the Wisconsin Alumni Research Foundation and in part by a National Science Foundation Departmental Instrument Grant (No. 28233), which allowed the purchase of the automated diffractometer. The authors also thank Mr. William B. Jensen for the many stimulating discussions.

Registry No. $ZrCl_3$, 10241-03-9; $ZrBr_3$, 24621-18-9; ZrI_3, 13779-87-8.

Supplementary Material Available: A listing of structure factor amplitudes for these compounds (8 pages). Ordering information is given on any current masthead page.

Contribution from the Science Research Laboratory, 3M Central Research Laboratories, St. Paul, Minnesota 55101

Partially Oxidized Cation Radical Complexes of Platinum(II)

A. R. SIEDLE,* M. C. ETTER, M. E. JONES, G. FILIPOVICH, H. E. MISHMASH, and W. BAHMET

Received November 30, 1981

Metal complexes of the type L_2MCl_2 (M = Pd, Pt) were prepared from $KPtCl_3(C_2H_4)$ or $(PhCN)_2PdCl_2$ and the electrochemically active ligands (L) phenothiazine, phenoselenazine, and phenoxathiin. The stereochemistries of the compounds were deduced from vibrational spectra and X-ray powder diffraction data. From $KPtCl_3(C_2H_4)$ and phenoselenazine in acetonitrile were obtained both *trans*-bis(phenoselenazine)dichloroplatinum(II) and *cis*-bis(phenoselenazine)dichloroplatinum(II)–acetonitrile. This solvated cis isomer crystallizes in space group $Cmc2_1$ with a = 14.693 (4) Å, b = 16.341 (5) Å, c = 10.643 (8) Å, V = 2555 Å^3, Z = 4, D_c = 2.07 g cm^{-3}, and D_m = 2.0 g cm^{-3}. The structure, refined with 1061 reflections for which $I > 2\sigma(I)$, converged at at R = 0.05. The acetonitrile occupies a lattice site and is not coordinated to the metal. The two Pt–Se distances are 2.376 (2) and 2.400 (2) Å. The cis phenoselenazine ligands are nearly planar with dihedral angles through the Se–N vectors of 172.8 and 173.1°. Adjacent *c*-glide related molecules are packed so that a 3.48 Å interplanar spacing occurs between the coordinated phenoselenazine ligands on adjacent molecules. Iodine oxidation led to *trans*-$(PSZ)_2PtCl_2I_{4.0}$, *trans*-$(PSeZ)_2PtCl_2I_{3.5}$, and *cis*-$(PSeZ)_2PtCl_2I_{3.9}$, which had significantly greater electrical conductivity than the insulating precursors. Resonance Raman and X-ray photoelectron spectroscopies indicate that the hole sites are localized on the heterocyclic ligands and that the iodine is present predominantly as I_5^-.

Introduction

Partially oxidized compounds containing platinum(II), particularly the tetracyanoplatinates, have attracted considerable attention on account of their anisotropic electron transport properties.[1-3] In $Pt(CN)_4^{2-}$ derivatives, the cyanide ion can function as both a σ donor and a π acceptor. We have investigated the preparation and properties of related materials of the type L_2PtCl_2, where L is a neutral aromatic ligand which is both a good donor and capable of undergoing reversible electron-transfer reactions. This paper describes the synthesis and properties of a family of L_2MCl_2 compounds (M = Pd, Pt; L = phenothiazine, phenoselenazine, phenoxathiin), the crystal structure of one of these, *cis*-bis(phenoselenazine)dichloroplatinum(II)–acetonitrile, which reveals an unusual conformational change on complexation of the ligand, and partial oxidation reactions with iodine which afford cation radical complexes of platinum.

Results and Discussion

Synthesis and Properties of the Complexes. The ligands employed in this study were phenothiazine (PSZ), **1**, phenoselenazine (PSeZ), **2**, and phenoxathiin (POT), **3**. Phenothiazine (PSZ) and phenoselenazine (PSeZ) are particularly interesting ligands since (1) the ring chalcogen atom should serve as an effective donor site, (2) the ligand π^* system can back-bond with filled metal d orbitals, and (3) phenothiazine

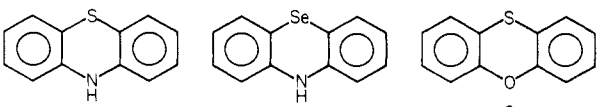

1 2 3

(1) "Extended Linear Chain Compounds", J. S. Miller, Ed., Plenum Press, New York, 1982.
(2) A. E. Underhill and D. M. Watkins, *Chem. Soc. Rev.*, 429 (1980).
(3) "Highly Conducting One-Dimensional Solids", J. T. Devreese, R. P. Evrard, and V. E. Van Doyen, Eds., Plenum Press, New York, 1979.

0020-1669/82/1321-2624$01.25/0

Table I. Analytical Data

	anal. calcd (found)				
	% C	% H	% N	% Cl	% other
trans-$(PSeZ)_2PtCl_2$ (4)	38.0	2.4	3.7	9.4	
	(38.2)	(2.3)	(4.2)	(9.4)	
cis-$(PSeZ)_2PtCl_2 \cdot CH_3CN$ (5)	39.0	2.6	5.3	8.9	
	(38.9)	(2.7)	(5.5)	(9.0)	
$(PSeZ)_2PdCl_2$ (6)	43.0	2.7	4.2		
	(43.4)	(2.9)	(4.5)		
$(PSZ)_2PtCl_2$ (7)	43.4	2.7	4.2	10.7	
	(43.3)	(2.9)	(4.5)	(10.7)	
$(PSZ)_2PdCl_2$ (8)	50.1	3.2	4.9	10.6	
	(49.8)	(3.1)	(5.2)	(10.5)	
$(PSZ)_2PdBr_2$ (9)	43.4	2.7	4.2		24.1
	(43.0)	(2.6)	(4.6)		(24.5) Br
$(POT)_2PtCl_2$ (10)	43.2	2.4		10.7	
	(42.6)	(2.3)		(10.8)	
$(POT)_2PdCl_2$ (11)	49.9	2.8		12.3	11.1
	(49.8)	(2.6)		(12.1)	(11.1) S
$(2\text{-}CH_3OPSZ)_2PdCl_2$ (12)	49.1	3.5	4.4		
	(48.6)	(3.3)	(4.7)		
$(2\text{-}ClPSZ)_2PdCl_2$ (13)	44.7	2.5	4.3	22.1	
	(45.0)	(2.2)	(4.3)	(21.7)	
$(PSZ)_2PtCl_2I_{4.0}$ (14)	24.6	1.5	2.4	6.1	43.3
	(23.9)	(1.8)	(2.5)	(5.8)	(43.9) I
trans-$(PSeZ)_2PtCl_2I_{3.5}$ (15)	24.0	1.3	2.3	6.0	37.0
	(24.4)	(1.6)	(2.5)	(6.2)	(37.3) I
cis-$(PSeZ)_2PtCl_2I_{3.9}$ (16)	23.0	1.3	2.2	5.7	39.6
	(23.0)	(1.3)	(2.3)	(6.0)	(39.2) I

Table II. Electronic Spectral Data

compd	λ_{max}, nm	compd	λ_{max}, nm
4	304, 462	11	290, 350 (sh), 470
5	300, 470	12	260, 316, 640
6	255, 330, 370, 600	13	255, 330, 625
7	240, 260, 300, 458	14	380, 425, 775
8	252, 326, 336, 633	15	260, 385, 440, 730
9	260, 360 (sh), 625	16	275, 310, 420, 775
10	290, 365		

reversibily forms a stable cation radical.[4,5]

The coordination chemistry of phenothiazine has not been thoroughly explored. It is known, however, that in the $PdCl_3^-$ complex of protonated 10-[2-(dimethylamino)propyl]phenothiazine, the heterocycle is bonded to the metal through the sulfur atom.[6] Phenothiazine forms charge-transfer complexes with 1,3,5-trinitrobenzene,[7] pyromellitic dianhydride,[8] and tetracyanoquinodimethan,[9] and the novel ion radical molecular complex with $[(CF_3)_2C_2S_2]_2Ni$ has been characterized by spectroscopic[10] and crystallographic[11] techniques.

The platinum compounds described here were obtained by reaction of $KPtCl_3(C_2H_4)$ and **1–3** in acetonitrile at room temperature. The desired L_2PtCl_2 compounds precipitated in analytically pure form. The analogous palladium derivatives were obtained by displacement of benzonitrile from $(PhCN)_2PdCl_2$. Analytical and spectroscopic properties for these compounds are given in Tables I, II, and S-1. Empirically, we find that the chalcogen donors **1–3** displace both ethylene and chloride ion from $PtCl_3(C_2H_4)^-$ regardless of the ratio of reactants employed. The presumably less basic donor phenazine, however, yields only *trans*-(phenazine)dichloro(ethylene)platinum(II).[12] The difference may also be related to the conformation of the free ligands: **1–3** are folded about the axis passing through the heteroatoms in the 9, 10 positions whereas phenazine is planar. This folding may relieve nonbonded interactions between peri hydrogens on adjacent ligands or between the chlorine atoms and the peri hydrogens. X-ray photoelectron spectra (ESCA) of the phenothiazine and phenoselenazine complexes of $PtCl_2$ (Table III) demonstrate that the chalcogen core binding energies increase by 1–1.5 eV on going from the free ligand to the metal adduct whereas the changes in the N(1s) levels are much smaller, 0.1–0.2 eV. This indicates that phenothiazine and phenoselenazine bind to platinum through the chalcogen atom. This mode of bonding is in contrast to that of thiazole and isothiazole, which are reported to coordinate to $Cr(CO)_5$ and $W(CO)_5$ solely through the nitrogen atom.[13]

When acetonitrile solutions of **2** and $KPtCl_3(C_2H_4)$ are combined, microcrystalline orange *trans*-$(PSeZ)_2PtCl_2$ (**4**) rapidly separates. This compound exhibits a single Pt–Cl stretching band at 325 cm^{-1}, cf. Table S-1, which is indicative of trans stereochemistry. On standing, the mother liquor slowly deposits large crystals of *cis*-$(PSeZ)_2PtCl_2 \cdot CH_3CN$ (**5**), whose infrared spectrum reveals two Pt–Cl stretching bands at 310 and 285 cm^{-1} and a band at 2260 cm^{-1} due to the lattice acetonitrile. The cis sterochemistry deduced from the infrared spectrum is confirmed by the X-ray study described below. This cis isomer **5** is evidently the thermodynamically more stable form as recrystallization of **4** from hot acetonitrile affords **5** along with some decomposition products as judged from infrared spectra and X-ray powder diffraction analysis. The palladium analogue, *trans*-$(PSeZ)_2PdCl_2$ (**6**), also shows a single ν_{Pd-Cl} band at 335 cm^{-1} and accordingly is formulated as the trans isomer. In agreement with this, X-ray powder patterns show that **4** and **6** are isomorphous.

The phenothiazine complexes $(PSZ)_2PtCl_2$ (**7**) and $(PSZ)_2PdCl_2$ (**8**) are assigned a cis stereochemistry on the basis of the presence of two metal–chlorine stretching bands at 340, 325 and 315, 280 cm^{-1} in **7** and **8**, respectively. The corresponding M–Cl bands in the Raman spectra occur at 360, 330 and 325, 285 cm^{-1}. The assignment of the 315- and 280-cm^{-1} absorptions to Pd–Cl modes is substantiated by their absence in the corresponding palladium bromide adduct, $(PSZ)_2PdBr_2$ (**9**). X-ray powder patterns showed that **7** and **8** are isomorphous with each other but not with **4** or **9**.

The metal–chlorine vibrations in the phenoxathiin complexes $(POT)_2PtCl_2$ (**10**) and $(POT)_2PdCl_2$ (**11**) are very weak in the infrared, but strong Raman bands occur in these compounds at 350, 330 and 330, 290 cm^{-1}, respectively, indicative of cis stereochemistry. These two compounds are also isomorphous with each other but not with the corresponding phenothiazine or phenoselenazine complexes.

The electronic spectra of the palladium and platinum complexes of **1** and **2** show interesting effects as the metal is varied. The longest wavelength bands in the platinum derivatives **4**, **5**, and **7** occur at 460 nm, but in the analogous palladium materials **6** and **8**, the lowest energy transitions are at 600 and 630 nm, respectively. This trend is similar to that observed in palladium and platinum complexes of tetrathiafulvalene (TTF) of the type $(TTF)_2MX_2$ (M = Pd, Pt; X = Cl, Br).[14,15] The longest wavelength band is attributed to a ligand → metal charge-transfer process which occurs at lower energy in the palladium compounds because of a closer match between

(4) E. Pellizzetti and E. Mentasti, *Inorg. Chem.*, **18**, 583 (1979).
(5) C. Bodea and I. Silberg, *Adv. Heterocycl. Chem.*, **9**, 322 (1968).
(6) W. J. Geary, N. J. Mason, L. A. Nixon, and I. W. Nowell, *J. Chem. Soc., Chem. Commun.*, 1064 (1980).
(7) C. J. Fritchie, Jr., *J. Chem. Soc. A*, 1328 (1969).
(8) R. Anthonj, N. Karl, B. E. Robertson, and J. Stezkowski, *J. Chem. Phys.*, **72**, 1244 (1980).
(9) H. Kobayashi, *Acta Crystallogr., Sect. B*, **B30**, 1010 (1974).
(10) W. E. Geiger, Jr., and A. H. Maki, *J. Phys. Chem.*, **75**, 2387 (1971).
(11) A. Singhabhandhu, P. D. Robinson, J. H. Fang, and W. E. Geiger, Jr., *Inorg. Chem.*, **14**, 1318 (1975).
(12) A. R. Siedle and F. J. Palensky, manuscript in preparation.
(13) K. H., Pannell, C. C. Lee, C. Parkanyi, and R. Redfern, *Inorg. Chem. Acta*, **12**, 127 (1975).
(14) A. R. Siedle, G. A. Candela, T. F. Finnegan, R. P. Van Duyne, T. Cape, G. F. Kokoszka, P. M. Woyciesjes, J. A. Hashmall, M. Glick, and W. P. Ilsley, *Ann. N.Y. Acad. Sci.*, **313**, 377 (1978).
(15) A. R. Siedle in "Extended Linear Chain Compounds", Vol. 2, J. S. Miller, Ed., Plenum Press, New York, p 469.

Table III. X-ray Photoelectron Spectroscopic Data

compd	binding energy, eV[a,b]							
	N(1s)	S($2p_{3/2}$)	S($2p_{1/2}$)	Se($3p_{3/2}$)	Se($3p_{1/2}$)	Cl($2p_{3/2}$)	Cl($2p_{1/2}$)	Pt($4d_{5/2}$)	I($3d_{5/2}$)
1	400.3	164.4	165.7						
2	400.2			161.9	168.0				
4	400.2			163.5	169.1	199.0	200.5	316.4	
7	400.7	165.5	167.6			199.7	201.2	316.7	
14	400.1	164.0	165.4			199.0	200.3	316.7	619.3
15	400.1			163.5	169.3	198.7	200.3	316.9	619.7
16	400.1			163.4	169.0	198.7	200.3	316.9	619.5

[a] ±0.1 eV. [b] Relative to C(1s) = 285.1 eV with FW et al. = eV.

vacant metal d orbitals and filled ligand π orbitals. In both classes of compounds, the ligands phenothiazine, phenoselenazine, and tetrathiafulvalene have relatively low ionization potentials and form stable cation radicals. The LMCT assignment in the L_2PdCl_2 system is supported by the observation that in the series bis(2-X-phenothiazine)dichloropalladium(II), the long wavelength band shifts to lower energy as the substituent X becomes more electron releasing and better able to stabilize a positive charge on the ligand in the photoexcited state. Thus, λ_{max} for **12** (X = CH_3O), **6** (X = H), and **13** (X = Cl) are 640, 630, and 625 nm, respectively.

Partially Oxidized Platinum Complexes. Exposure of orange microcrystalline *trans*-$(PSZ)_2PtCl_2$ to iodine vapor at 50 °C produces deep purple, noncrystalline *trans*-$(PSZ)_2PtCl_2I_{4.0}$ (**14**). Similarly, treatment of **4** and **5** with excess iodine produced the partially oxidized noncrystalline compounds *trans*-$(PSeZ)_2PtCl_2I_{3.5}$ (**15**) and *cis*-$(PSeZ)_2PtCl_2I_{3.9}$ (**16**). X-ray powder photographs disclosed that, when a deficiency of iodine was employed, the products gave a diffraction pattern with only one reflection at 9.3 Å and lines due to unreacted starting material. Therefore, the iodine oxidations appear to be stoichiometric and intermediate phases with an I:Pt ratio of less than 3.5:1 were not observed.

Lattice acetonitrile is lost upon iodination of *cis*-$(PSeZ)_2PtCl_2 \cdot CH_3CN$ as indicated by elemental analyses, loss of the C≡N stretching band at 2260 cm^{-1}, and the observation of acetonitrile as a volatile byproduct. It is tempting to suppose that the iodine in **16** may enter the lattice by way of the channels occupied by the acetonitrile. The iodinated phase acts as a barrier to the further diffusion of iodine into the crystal lattice. Experiments with crystals of **5** always yielded materials with a deficiency of the iodine dopant in the interior of the crystals. This was clearly visualized by electron microprobe analyses in which crystals were exposed to iodine vapor and then mounted in epoxy cement and cross sectioned with a microtome. The Pt:Se:Cl:I ratio in the outer portion of the crystals was close to the 1:2:2:4 values indicated by bulk chemical analyses, but in the interior of the samples, the iodine content was much lower.[16] The iodination reactions are at least partially reversible, and the TGA curves of **14–16** exhibited sharp breaks at 160, 175, and 300 °C, respectively, corresponding to weight losses of 30, 17, and 9%. Elemental iodine could be seen on the cold walls of the TGA apparatus and was identified by mass spectroscopy.

Spectroscopic measurements provide important characterization data on these iodinated compounds. Hydrogen iodide is not formed during the preparative reactions, and the infrared spectra of **15–17** are quite similar to those of their precursors. This indicates that iodination of the aromatic rings has not occurred for such substitution would be expected to lead to significant changes in the ring-breathing modes[5] and to the formation of hydrogen iodide. Further, the X-ray photoelectron spectra disclose a shift of the platinum $4d_{5/2}$ core levels of only about 0.5 eV to higher energy (cf. Table III). This shift is too small to be consistent with oxidation of Pt(II) to Pt(IV). For example, the difference in Pt($4f_{7/2}$) binding energies in K_2PtCl_6 and K_2PtCl_4 is 2.5 eV.[17] Resonance Raman spectra of **15–17** reveal strong bands at 161 cm^{-1} due to I_5^- and much weaker scattering at 108 cm^{-1} due to small amounts of I_3^-.[18] We conclude, therefore, that iodination of L_2PtCl_2 produces salts in which the ligand is oxidized and the resulting cation radical is coordinated to platinum(II) so that **15**, for example, is formulated as $[(PSZ)_2PtCl_2]^{0.8+}(I_5)_{0.8}$.

Table IV. Electron Spin Resonance and Conductivity Data

compd	g[a]	ΔH, G	A/B	spins/g	σ, $(\Omega\ cm)^{-1}$
$(PSZ)_2PtCl_2I_{4.0}$	2.0072	14	1.0 (3)	1.3×10^{19}	2×10^{-7}
trans-$(PSeZ)_2PtCl_2I_{3.5}$	2.0203	30	1.32	7.3×10^{18}	3×10^{-7}
cis-$(PSeZ)_2PtCl_2I_{3.9}$	2.0210	30	1.24	9×10^{18}	2×10^{-5}

[a] ±0.0002; average g value—$g_\parallel$ and $g_\perp$ were not resolved.

Electron spin resonance spectra of **15** and **16**, summarized in Table IV, show broad peaks at $g \simeq 2.02$; ΔH (peak to peak) is about 30 G. The resonances have asymmetry parameters of about 1.24. The g values for these compounds are fairly close to the free electron value and are indicative of ligand-centered hole sites. The ESR signal from **14** was much sharper and more symmetrical than those from the iodinated phenoselenazine analogues, and its g value is much closer to the free electron value. A metal-centered cation radical would be expected to exhibit a much larger g value and, for example, $g_\parallel = 2.29$ and $g_\perp = 2.11$ have been reported for the cation (phthalocyanine)nickel(III).[19] For this reason, we conclude that, in agreement with the X-ray photoelectron spectroscopic data, $(PSZ)_2PtCl_2$ and $(PSeZ)_2PtCl_2$ undergo partial oxidation with iodine to give materials containing complexed, ligand-centered holes and that there is not significant spin density on platinum.

The spin concentrations in the partially oxidized L_2PtCl_2 compounds were measured by integration of the first derivative EPR spectra. The values, normalized to spins per mole of I_5^-, are significantly lower than the values calculated assuming the creation of one unpaired electron per I_5^-. This effect may arise from spin pairing between adjacent cation radicals in the solid, a phenomenon observed in other cation radical salts such as $(TTF)(BF_4)_{0.67}$. In partially oxidized $(PSZ)_2PtCl_2$, the spins to moles of I_5^- ratio increases as the amount of iodine incorporated in the sample is decreased. Under these conditions, where **7** persists as a separate phase, greater separation be-

(16) Electron microprobe analysis has recently been used to map AsF_5 dopant profiles in conducting complexes of polyphenylene sulfide: L. W. Shacklette, R. L. Eisenbaumer, R. R. Chance, H. Eckhardt, J. E. Frommer and R. H. Baughman, *J. Chem. Phys.*, **75**, 1919 (1981).

(17) W. M. Riggs in "Electron Spectroscopy", D. A. Shirley, Ed., North-Holland Publishing Co, London, 1972, p 713.

(18) C. J. Schramm, R. P. Scaringa, D. R. Stojakovic, B. M. Hoffman, J. A. Ibers, and T. J. Marks, *J. Am. Chem. Soc.*, **102**, 6702 (1980). This reference describes the use of resonance Raman spectroscopy, and of many other techniques, in the characterization of partially oxidized materials.

(19) A. P. Bobrovski and A. N. Sidorov, *J. Struct. Chem.* (*Engl. Trans.*), **17**, 50 (1976).

Table V. Positional and Thermal Parameters[a] and Their Estimated Standard Deviations

atom	x	y	z	B_{11}	B_{22}	B_{33}	B_{12}	B_{13}	B_{23}
Pt	0.0000 (0)	0.19471 (8)	0.5004 (3)	5.05 (5)	2.92 (4)	4.11 (4)	0	0	0.14 (7)
Se1	0.0000 (0)	0.1370 (2)	0.7053 (4)	7.0 (2)	2.9 (1)	4.7 (2)	0	0	0.1 (1)
Se2	0.0000 (0)	0.0607 (2)	0.4082 (4)	9.5 (3)	3.3 (1)	4.0 (2)	0	0	−0.2 (1)
Cl1	0.0000 (0)	0.2476 (6)	0.298 (1)	6.4 (5)	4.6 (4)	4.8 (4)	0	0	−0.0 (4)
Cl2	0.0000 (0)	0.3258 (5)	0.578 (1)	8.4 (6)	3.0 (3)	5.6 (5)	0	0	−0.6 (4)
N1	0.0000 (0)	0.280 (2)	0.918 (3)	4 (1)	5 (1)	4 (1)	0	0	1 (1)
N2	0.0000 (0)	−0.098 (2)	0.588 (3)	3 (1)	5 (1)	5 (1)	0	0	−1 (1)
N3	0.0000 (0)	0.427 (2)	0.084 (3)	B_{iso} = 5.0 Å^2					
C1	0.085 (2)	0.250 (1)	0.884 (2)	7 (1)	3.0 (9)	2.7 (9)	−0 (1)	−1 (1)	1.2 (8)
C2	0.159 (2)	0.286 (2)	0.948 (3)	5 (1)	5 (1)	7 (1)	−1 (1)	0 (1)	2 (1)
C3	0.248 (3)	0.259 (2)	0.918 (4)	8 (2)	4 (1)	11 (2)	−1 (1)	−1 (2)	2 (2)
C4	0.260 (2)	0.193 (2)	0.821 (3)	6 (1)	6 (1)	12 (2)	0 (1)	−1 (2)	5 (1)
C5	0.182 (2)	0.159 (2)	0.761 (3)	5 (1)	5 (1)	5 (1)	1 (1)	1 (1)	2 (1)
C6	0.098 (2)	0.187 (1)	0.794 (2)	8 (1)	3.4 (9)	2.7 (8)	−0 (1)	−0 (1)	1.1 (9)
C7	0.099 (7)	0.005 (1)	0.490 (2)	0 (1)	2.5 (7)	0 (1)	1.5 (9)	0 (1)	0.1 (9)
C8	0.190 (2)	0.033 (2)	0.464 (3)	8 (2)	5 (1)	7 (2)	−2 (1)	2 (1)	−2 (1)
C9	0.264 (2)	−0.006 (2)	0.522 (4)	8 (1)	6 (1)	7 (2)	2 (1)	1 (2)	−1 (2)
C10	0.248 (2)	−0.076 (2)	0.592 (3)	8 (2)	6 (1)	6 (1)	1 (2)	−1 (2)	−3 (1)
C11	0.163 (2)	−0.104 (2)	0.611 (3)	5 (1)	5 (1)	6 (1)	0 (1)	−0 (1)	−3 (1)
C12	0.084 (2)	−0.066 (1)	0.562 (2)	7 (1)	5 (1)	2.5 (8)	1 (1)	−1 (1)	−3.0 (8)
C14	0.0000 (0)	0.457 (2)	0.184 (4)	B_{iso} = 5.0 Å^2					
C13	0.0000 (0)	0.487 (2)	0.305 (4)	B_{iso} = 5.0 Å^2					

[a] The form of the anisotropic thermal parameter is $\exp[-1/4(B_{11}h^2a^{*2} + B_{22}k^2b^{*2} + B_{33}l^2c^{*2} + 2B_{12}hka^*b^* + 2B_{13}hla^*c^* + 2B_{23}klb^*c^*)]$.

tween radical sites should occur, leading to less effective spin pairing at lower iodine concentrations.

The neutral complexes **4**, **5**, and **7** are insulators, with conductivities estimated at $\leq 10^{-11}$ $(\Omega\ cm)^{-1}$. The partially oxidized, iodinated analogues **14–16** exhibit significantly higher conductivities and may be considered as semiconductors (cf. Table V). The conductivity of *cis*-$(PSeZ)_2PtCl_2I_{3.9}$ is the highest of the compounds studied, 2×10^{-5} $(\Omega\ cm)^{-1}$. In this material, the close overlap of the phenoselenazine rings observed in the structure of *cis*-$(PSeZ)_2PtCl_2$ may provide an additional mechanism for electron transport. In this regard, Matsunaga and co-workers have described conducting complexes of phenothiazine and iodine.[20-22]

Structure of *cis*-$(PSeZ)_2PtCl_2 \cdot CH_3CN$. The crystal and molecular structures of **5** were determined in order to more thoroughly characterize the L_2PtCl_2 compounds.

Figures 1 and 2 show the molecular geometry, selected distances and angles, and unit cell packing pattern. The molecule is mirror symmetric with all heavy atoms, the nitrogen, and the acetonitrile molecule on the $x = 0$ plane. The two Pt–Se distances, 2.376 (2) and 2.400 (2) Å, are shorter than the 2.430 (2) Å separation found in *trans*-bis(1,4-oxaselanan)dibromoplatinum(II).[23] The shortest contact with the noncoordinating lattice acetonitrile is 3.7 Å between chlorine and the nitrile carbon. The phenoselenazine groups are seen to be nearly planar, and, indeed, the maximum atomic displacement from the three ring plane containing Se(1) is 0.012 Å and from that containing Se(2) is 0.036 Å. In the recently reported structure of uncomplexed phenoselenazine,[24] it was found that this molecule is folded with a dihedral butterfly angle of 169.6°, much like that of phenothiazine (dihedral angle = 153.3 and 158.5° in different polymorphs[25]). In **5**, the two phenoselenazine ligands are nearly planar with dihedral angles of 172.8 and 173.1°. Such flattening of the

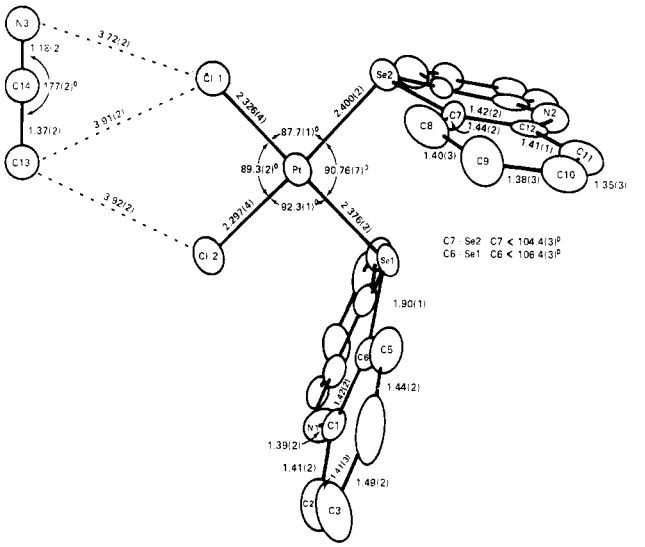

Figure 1. Molecular dimensions of *cis*-$(PSeZ)_2PtCl_2 \cdot CH_3CN$, viewed along [100].

ligand rings upon binding to a heavy metal appears not to be a general phenomena. For example, coordination of gold to sulfur in thianthrene produces only a small conformational effect. The dihedral angles through the S–S axis in thianthrene[26] and (thianthrene)trichlorogold(III)[27] are 128.1 and 129.5°, respectively.

This usual conformation is all the more striking when one considers that adjacent *c*-glide related molecules are packed such that a short (3.48 Å) interplanar spacing occurs between the ligands on neighboring molecules. This spacing is indicative of a possible charge-transfer interaction occurring between the molecules and compares well with the 3.50-Å separation observed in the molecular complex of anthracene and tetracyanoquinodimethan.[28] The spacing between donor phenothiazine and acceptor $[(CF_3)_2C_2S_2]_2Ni$ in the DDAA stacking sequence in their crystalline complex is 3.36 Å. In this compound, phenothiazine exists predominantly as a

(20) T. Matsumoto and Y. Matsunaga, *Bull. Chem. Soc. Jpn.*, **54**, 568 (1981).
(21) T. Matsumoto and Y. Matsunaga, *Bull. Chem. Soc. Jpn.*, **43**, 2007 (1970).
(22) S. Doi and Y. Matsunaga, *Bull. Chem. Soc. Jpn.*, **48**, 3747 (1975).
(23) J. C. Barnes, G. Hunter, and M. Lown, *J. Chem. Soc., Dalton Trans.*, 458 (1972).
(24) P. Villares, R. Jiminez-Garay, A. Conde, and R. Marques, *Acta Crystallogr., Sect. B.*, **B32**, 2293 (1976).
(25) R. M. Williams and S. C. Wallwork, *Acta Crystallogr., Sect. B*, **B24**, 168 (1968).
(26) I. Rowe and B. Post, *Acta Crystallogr.*, **11**, 373 (1958).
(27) N. W. Alcock, K. P. Aug, K. F. Mok, and S. T. Tau, *Acta Crystallogr., Sect. B*, **B34**, 3364 (1978).
(28) G. D. Andreeti, G. Bocelli, and P. Sgarabotto, *Acta Crystallogr., Sect. B*, **B36**, 1839 (1980).

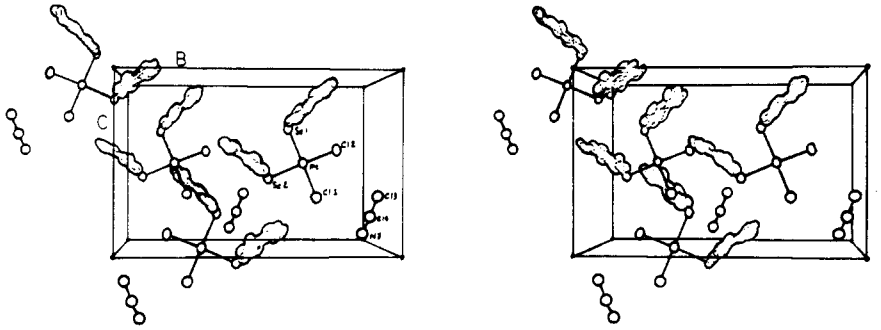

Figure 2. Stereoview of the unit cell of *cis*-$(PSeZ)_2PtCl_2 \cdot CH_3CN$, viewed along [100].

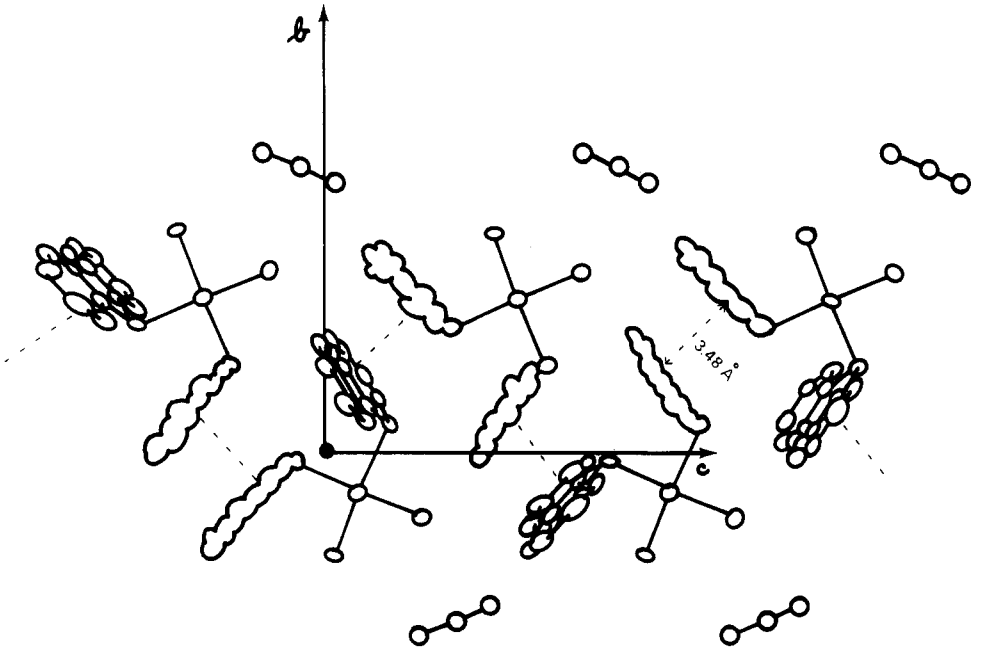

Figure 3. Packing of the molecules along the *c* axis showing the 3.48 Å contact (dotted line) between the phenoselenazine ligands in neighboring glide-related molecules.

nonplanar cation radical with a dihedral angle of approximately 172°.[11] Donor–acceptor spacing in the phenothiazine–trinitrobenzene charge-transfer complex is 3.37 Å, and the heterocycle is again folded with an average dihedral angle of about 165–172°.[7] It would appear that there is a low-energy barrier associated with changes in the dihedral angle and that packing forces are significant determinants of phenothiazine conformation in crystalline solids.[28] In the case of *cis*-$(PSeZ)_2PtCl_2 \cdot CH_3CN$, this π–π mode of interaction between the severely flattened phenoselenazine rings leads to a one-dimensional interaction propagating along the *c*-axis of the crystal as shown in Figure 3. The intramolecular separation between selenium atoms in phenoselenazine ligands in neighboring $(PSeZ)_2PtCl_2$ units is 3.89 Å, somewhat shorter than the sum of the van der Waals radii (4.0 Å), which may be indicative of a weak chalcogen–chalocogen interaction as well. Either of these bonding forces, if they persist, may provide a mechanism for anisotropic electron transport in the partially oxidized *cis*-$(PSeZ)_2PtCl_2I_{3.9}$ (**16**), in agreement with the conclusions of Marks and others[1,2,3,29] that control of lattice architecture is crucial in synthesis of conductive, low-dimensional materials.

Experimental Section

Infrared and optical spectra were obtained on Nujol mulls of the samples on Perkin-Elmer 283 and Cary 14 spectrometers. Raman spectra were recorded on a Spex Ramalog instrument using 5145-Å excitation. X-ray powder patterns were obtained with a General Electric diffraction camera with 14.32-cm film diameter, using 40-keV copper radiation. Intensities were estimated visually. A Perkin-Elmer TGS-1 thermal analysis system was used to record TGA data in air with heating rates of 10 °C/min. The X-ray photoelectron spectra were obtained with a Hewlett-Packard 5950B spectrometer and monochromatized Al Kα X-rays (E = 1486.6 eV). The data were accumulated on a HP 21MX computer and were plotted in digital form. The C(1s) photoelectron line was taken as an internal standard with E_b = 285.0 eV.

EPR data were recorded on a Varian V-4502 EPR spectrometer with a 9-in. magnet, equipped with Fieldial magnetic field regulation and control. Resonance frequency was measured by a Hewlett-Packard Model X532B microwave frequency meter. Single EPR lines of different widths and symmetry (Table V) were recorded at 100-kc modulation frequency. Experimental g values were determined by taking the field values of the base line crossing by derivative lines and (by use of a TE102 dual microwave cavity) comparing them to the field value of the central line (g = 2.0055) of the triplet spectrum of a peroxylaminedisulfonate reference solution. Spin concentration (spins/g) were determined by comparison of integrated areas of absorption curves with those for an intensity standard (SRM-2601 of NBS). Base-line correction that was linear to the first integral was used. Precautions were taken to keep filling factors of the samples and the reference comparable and to account for the anisotropy of the ruby standard.

Conductivity measurements were made on compressed pellets by the two-probe technique.

Acetonitrile was distilled from calcium hydride before use. Phenothiazine was recrystallized from ethanol and then sublimed under

(29) C. W. Dirk, E. A. Mintz, K. F. Schoch, Jr., and T. J. Marks, *J. Macromol. Sci., Chem.*, **A16**, 275 (1981), and references cited therein.

vacuum. Phenoselenazine was sublimed under high vacuum and then chromatographed on an alumina column, eluting with acetonitrile.

***trans*-$(PSeZ)_2PtCl_2$ (4) and *cis*-$(PSeZ)_2PtCl_2 \cdot CH_3CN$ (5).** Solutions of 1.11 g (3 mmol) of $KPtCl_3(C_2H_4)$ in 15 mL of acetonitrile and 1.39 g of phenoselenazine (6 mmol) in 100 mL of warm acetonitrile were combined with stirring. After 30 min, orange microcrystalline **4** was collected on a filter. The mother liquor was allowed to stand for 24 h, after which time the large orange needle crystals of **5** which had separated were isolated by filtration. Both compounds were washed with acetonitrile, water, and then with acetonitrile and dried under vacuum. The yields of **4** and **5** were 1.04 and 0.85 g, respectively.

$(PSZ)_2PdCl_2$ (8). A solution of 0.38 g (1 mmol) of bis(benzonitrile)dichloropalladium(II) in 20 mL of acetonitrile was added to 0.40 g (2 mmol) of phenothiazine in 10 mL of the same solvent. After 1.5 h, the copper-colored crystals which had deposited from the violet reaction mixture were collected on a frit and washed with fresh solvent. After the crystals were vacuum-dried, the yield was 0.56 g.

The other complexes listed in Table I were similarly prepared.

Iodination of *cis*-$(PSeZ)_2PtCl_2 \cdot CH_3CN$. Iodination reactions were carried out in a Y-shaped reaction vessel. Two of the arms were fitted with glass bulbs attached by standard taper joints. In one of the arms was placed a coarse glass frit so that solid iodine would not come into contact with the platinum compound. The third arm was fitted with a stopcock and a joint so that the apparatus could be attached to a vacuum line.

A 0.20-g (0.25-mmol) sample of **5** and 0.13 g (1.0 mmol) of iodine were placed in separate bulbs. The bulb holding the iodine was cooled with liquid nitrogen while the apparatus was evacuated. After the stopcock was closed, the reaction vessel was removed from the vacuum line and placed in a 50 °C oven. After 15 h, it was reattached to the vacuum line and the volatile products were removed through a fractionation train. Unreacted iodine was retained in a 0 °C trap. Other volatiles were redistilled from a drop of mercury. GC–MS analysis revealed that 0.2 mmol of acetonitrile and no hydrogen iodide had been produced. The purple, solid iodination product was subjected to continuous pumping at 25 °C for 8 h to remove any losely held iodine. The weight of the product, **16**, was 0.31 g, indicating the formula $(PSeZ)_2PtCl_2I_{3.9}$.

Similar techniques were employed to produce **14** and **15**.

Crystal Structure Determination

Crystallization of **5** from hot acetonitrile gave bright red oblong crystals with average dimensions of 0.24 × 0.08 × 0.02 mm. Weissenberg and film methods were used to determine the space group and unit cell dimensions. Extinctions $h0l$ (l odd), $0kl$ (k, l odd), $hk0$ ($(h + k)$ odd), and hkl ($(h + k)$ odd) were consistent with $Cmcm$ or $Cmc2_1$. A Wilson plot gave acentric statistics, and the structure refined smoothly in space group $Cmc2_1$ with $Z = 4$.

Crystal Data: $PtSe_2Cl_2N_3C_{26}H_{19}$, $M_r = 797.4$, orthorhombic, $Cmc2_1$, $a = 14.693$ (4) Å, $b = 16.341$ (5) Å, $c = 10.643$ (8) Å, $V = 2555.5$ Å^3, $Z = 4$, $D_c = 2.07$ g cm^{-3}, $D_m = 2.0$ g cm^{-3}, $F(000) = 1504$, μ(Mo Kα) = 90.7 cm^{-1}. The needle axis of the crystal corresponds to the c axis.

Unit cell dimensions, determined on a Nonius CAD 4 diffractometer (Mo Kα, $\lambda = 0.7107$ Å by a least-squares fit to the settings for 25 reflections, gave a monoclinic unit cell which was transformed by a Delauney reduction to the orthorhombic unit cell that had been observed with film methods. Intensity data were collected in the octant hkl out to $2\theta = 50°$. A total of 1236 unique reflections was measured with 1061 above zero at the $2\sigma(I)$ confidence level. There was no evidence for crystal decomposition. Lorentz and polarization corrections were applied, but no correction was made for extinction or absorption.

The structure was solved with Patterson techniques. The Pt atom was located on the $x = 0$ mirror plane. A difference map, phased with Pt only, revealed a double image, in the mirror plane, of the Se, Cl, and N positions. One of these images was chosen and used in a structure factor calculation to give $R = 0.18$. All the other carbon atoms and the acetonitrile molecules were located by difference Fourier techniques. Full-matrix least-squares refinement of the positional and anisotropic thermal parameters (the acetonitrile thermal parameters were refined isotropically) converged with $R = 0.050$ and $R_w = 0.054$ on the basis of 1061 nonzero reflections.[30] The highest electron density on a final difference map was 0.95 e Å^{-3}. The final atomic coordinates are presented in Table V. Tables of structure factors and temperature factor expressions are available as supplementary material.

Acknowledgment. The authors are grateful to Professor T. J. Marks and C. W. Dirk, Department of Chemistry and Materials Research Center, Northwestern University, for assistance in obtaining the resonance Raman spectra and to members of the 3M Analytical and Properties Research Laboratory for physical and spectroscopic data.

Registry No. **1**, 92-84-2; **2**, 262-05-5; **3**, 262-20-4; **4**, 81447-18-9; **5**, 81496-24-4; **6**, 81447-19-0; **7**, 81447-20-3; **8**, 81447-21-4; **9**, 81447-22-5; **10**, 81447-23-6; **11**, 81447-24-7; **12**, 81447-25-8; **13**, 81447-17-8; $KPtCl_3(C_2H_4)$, 12012-50-9; $(PhCN)_2PdCl_2$, 14873-63-3.

Supplementary Material Available: Listings of final thermal parameters, structure factors, and infrared spectral data (Table S-1) (14 pages). Ordering information is given on any current masthead page.

(30) All calculations were carried out on a PDP 11/45 computer using the Enraf-Nonius SDP programs. The scattering curves were taken from the analytical expressions in the "International Tables for X-ray Crystallography", Kynoch Press, Birmingham, England. In the least-squares analysis the function minimized was $\sum w(|F_o| - |F_c|)^2$, where $w = 1$. The unweighted and weighted residuals are defined as $R = (\sum||F_o| - |F_c||)/\sum|F_o|$ and $R_w = (\sum w(|F_o| - |F_c|))^2/(w|F_o|)^2$.